5th Joint International Symposium on Deformation Monitoring (JISDM), 20-22 June 2022, Valencia, Spain
DOI: http://doi.org/10.4995/JISDM2022.2022.13907

High-rate real-time single-frequency PPP for structural motion detection in horizontal directions

Mert Bezcioglu[1], Baris Karadeniz[1], Cemal Ozer Yigit[1], Ahmet Anil Dindar[2], Burak Akpinar[3]

[1] Department of Geomatics Engineering, Gebze Technical University, Turkey, (mbezcioglu@gtu.edu.tr; b.karadeniz@gtu.edu.tr; cyigit@gtu.edu.tr)
[2] Department of Civil Engineering, Gebze Technical University, Turkey, (adindar@gtu.edu.tr)
[3] Department of Geomatics Engineering, Yildiz Technical University, Turkey, (bakpinar@yildiz.edu.tr)

Key words: *single-frequency PPP; real-time monitoring; structural health monitoring; GPS*

ABSTRACT

Thanks to advances in receiver and software technology, the high-rate GPS (Global Positioning System) technique has become very important in monitoring the dynamic behavior of man-made structures in both real-time and post-missions. Real-time monitoring of the changes in the behavior of structures due to effects such as natural disasters, wind effect, traffic loading is critical in order to take precautions in time. In this study, the performance of the Real-Time Single Frequency Precision Point Positioning (RT SF-PPP) method based on IGS (International GNSS Service) RTS (real-time stream) products to capture the behavior of dynamic motions was evaluated. The performance of the SF RT-PPP method to detect dynamic behaviors was evaluated based on 20 Hz single frequency GPS observations obtained from shake table experiments, including 10 mm amplitude and different oscillation frequencies including 0.1, 0.6, 1.0, 2.0 and 3.0 Hz. RT SF-PPP results were compared with reference LVDT (Linear Variable Differential Transformer) and relative (or double difference) GPS positioning both frequency and time domain. Results show that the high-rate RT SF-PPP method can capture the frequencies and amplitudes of harmonic motions and it is comparable to LVDT and Relative GPS positioning solutions. These results show that the high-rate RT SF-PPP method can monitor earthquake-induced real-time vibration frequencies and amplitudes, which is especially important for early warning systems.

I. INTRODUCTION

For high-precision structural displacement retrieval, high-rate GNSS has been widely employed. The advancements in GNSS receivers enable a wide variety of structural engineering applications. Therefore, high-rate GNSS PPP is an essential instrument for structural health monitoring applications. Because it does not require a reference GNSS station, the GNSS PPP technique has been developed and is widely used (Zumberge *et al.*, 1997; Kouba and Heroux, 2001). Using precise orbit and clock products, the PPP approach can provide position information with precision ranging from centimeters to decimeters (El-Mowafy *et al.*, 2017). Numerous studies on the high-frequency PPP technique have proven the method to be a cost-effective absolute positioning method for GPS seismology (Savage *et al.*, 2004; Calais *et al.*, 2006; Kouba, 2003; Avallone *et al.*, 2011; Xu *et al.*, 2013; Yigit *et al.*, 2016; Alcay *et al.*, 2019) and structural health monitoring (Moschas *et al.*, 2014; Yigit, 2016; Yigit and Gurlek, 2017; Kaloop *et al.*, 2018; Yigit *et al.*, 2020; Kaloop *et al.*, 2020; Yigit *et al.*, 2021).

The PPP approach commonly employs IGS Rapid or Final products, however they are provided to users at least 17 hours and two weeks after the previous observation, respectively (Wang *et al.*, 2018a). IGS also provides Ultra-Rapid products that are available two hours after the last observation, but these three products are not useful for real-time applications due to their latency. The PPP approach can be also employed in real-time with real-time precise satellite orbit and clock corrections. Earthquake-induced ground motions can be monitored instantaneously, and damage assessments can be performed rapidly using the real-time PPP approach. The Real-time GPS-PPP approach has recently applied to real bridge monitoring, and PPP-derived outcomes were compared to relative positioning results (Tang *et al.*, 2017). They demonstrated that Real-time PPP can be deployed as an alternate way to the relative method for monitoring man-made engineering structures. IGS provides real-time satellite orbit and clock products to users who want to obtain RT-PPP solutions through IGS RT Service (RTS). (Chen *et al.*, 2018; Wang *et al.*, 2018b; Bahadur, 2021). IGS also offers users combined real-time analysis products that allow post-mission PPP under real-time conditions. These products are provided to users at 10 s for clock and 30 s for orbit sampling interval, and they are derived from the IGC01 stream. The combined IGC01 orbit and clock products currently include GPS corrections (Defraigne *et al.*, 2015).

The RT-PPP approach based on combined IGC01 products was assessed in this investigation for capturing high-rate dynamic motions. Based on 20 Hz single-frequency GPS observations from shake table tests with different amplitude and frequency of

oscillations, the RT-PPP approach for detecting dynamic motions was evaluated. The results of the RT-PPP were compared to those of the reference relative GPS positioning and LVDT sensors.

II. BASICS OF PPP AND DESCRIPTION OF EXPERIMENTS

A. *Methodology*

The basic pseudorange and carrier-phase observation equations of GPS for PPP are as follows (Eqs. 1 and 2):

$$P = \rho + cdt_r + cdt^s + T + I + c(d_r - d^s) + e \quad (1)$$

$$\phi = \rho + cdt_r + cdt^s + T - I + c(\delta_r - \delta^s) + \lambda N + \varepsilon \quad (2)$$

where P = GPS pseudorange measurement in meters
ϕ = GPS carrier-phase measurement in meters
ρ = true geometric distance in meters
c = speed of light in vacuum
dt_r= clock errors for receiver
dt^s = clock errors for satellite
T = tropospheric component in meters
I= ionospheric component in meters
d_r = receiver's frequency-dependent code hardware delay in seconds
d^s = satellite's frequency-dependent code hardware delay in seconds
e = unmodelled residual errors and relevant system noise in meters for code observations
δ_r = receiver's frequency-dependent carrier-phase hardware delay in seconds
δ^s = satellite's frequency-dependent carrier-phase hardware delay in seconds
ε = unmodelled residual errors and relevant system noise in meters for phase observations
λ = the wavelengths of the carrier frequency in meters
N = integer ambiguity parameters in cycles

B. *Experiment design*

A shake table, which can generate the sinusoidal harmonic motion at various frequencies and amplitudes, was employed in this study to assess the detecting dynamic motions performance of high-rate real-time SF-PPP. The shake table is made up of three parts: a control unit that controls the frequency and amplitude of dynamic motions, a reference table from which movements are generated, and a motion table that travels in a single axis. Figure 1 shows the shake table employed in this study's tests. The GNSS receiver is placed on a black flat plate, which has a190 mm total stroke and moves within 95 mm in the uniaxial direction. The table motion is provided by an electric system that produces negligible oscillations and has a maximum speed of 400 mm/s. The position of the table is validated using an LVDT integrated beneath the motion table. Moreover, the LVDT sensor in the table can collect data at 100 Hz sampling rate, provide precision at mm level, and is controlled by computer software.

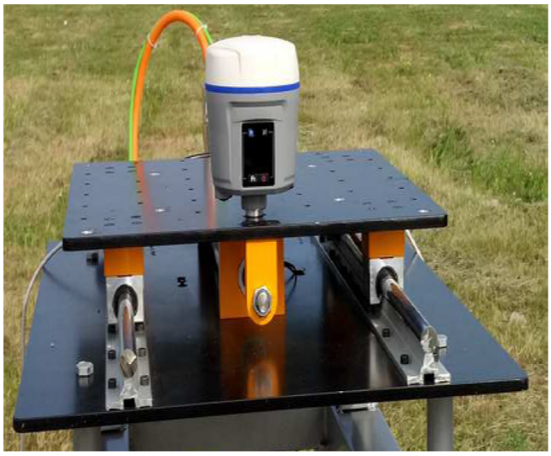

Figure 1. Employed shake table and GPS receiver in experiments.

Five harmonic motion cases with various amplitudes and frequencies generated by the shake table and detailed in Table 1 were chosen to examine the performance of SF-PPP in structural health monitoring applications. As shown in Table 1, 5 harmonic motions with frequencies ranging from 0.1 to 3.0 Hz and amplitudes of 5 mm were simulated.

Table 1. The frequency and amplitude of oscillations in each case chosen for this investigation

Frequency of Motions	Amplitude of Motions 10 mm
0.1 Hz	Case 1
0.6 Hz	Case 2
1.0 Hz	Case 3
2.0 Hz	Case 4
3.0 Hz	Case 5

C. *Processing strategy*

Two dual-frequency CHC I80 GNSS receivers are used in this investigation and GPS observations were collected with 10° cut-off angle at 20 Hz sampling rate and. One GNSS receiver collected the data for the PPP solution on the shake table, while the other GNSS receiver was placed at a known point to perform a relative positioning solution approximately 60 m from the shake table. The tests lasted approximately one hour, and were conducted at the Gebze Technical University campus in Gebze. During the experiment, 7 to 9 GPS satellites were observed. RTKLIB 2.4.2, an open-source library, was used to process single-frequency only-GPS data for relative positioning (Takasu and Yasuda, 2009). gLAB v5.5.1 software was used to implement SF-PPP solutions based on IGS-RT products (Ibáñez *et al.*, 2018). Displacements in the North and East directions derived from both relative positioning and RT-PPP are projected onto the

movement direction of the shake table as defined by Yigit *et al.* (2021).

III. Results and Discussion

Evaluation of the results obtained from the SF-PP method from harmonic motion experiments in various frequency and amplitude ranges is discussed in this section. To validate the performance of the high-rate RT SF-PPP, LVDT data and only-GPS SF-RP data were used as a reference in all experiments. The displacement time series of the north and east components derived from the SF-RP (top) and SF RT-PP (second from top) for harmonic oscillations are shown in Figure 2. The displacements derived from the SF-PPP methods have some low frequency fluctuations and trends in the long and short term for both components, whereas the time series of SF-RP are very consistent. Since the structural health monitoring applications focus on short-term dynamic movements of one minute or less, low-frequency components are not a problem. Moreover, various filtering techniques can successfully eliminate these short- and long-term oscillations. To remove the long-term fluctuations, all GNSS-based techniques' time series were filtered using a fifth-order Butterworth high-pass filter. For the first example, different cut-off frequencies were used, and for the next four cases, different cut-off frequencies were used. The purpose for using two separate cut-off frequencies was that when the entire time series was evaluated by FFT, unexpected peak frequencies between 0.1 Hz and 0.3 Hz were detected. As a result, the cut-off frequency of the filter for Case 1 was 0.08 Hz, whereas the cut-off frequency for all other cases was 0.20 Hz. The time series obtained as a result of the filter applied to SF-RP (third from top) and SF RT-PPP (fourth from top) solutions used in this paper can be seen in Figure 2. The figure demonstrates that after applying the high pass filter, the long-term components in the displacement time series obtained from SF RT-PPP solutions are eliminated. It is obvious, in particular, that the SF-PPP method is strongly compatible with the SF-RP time series.

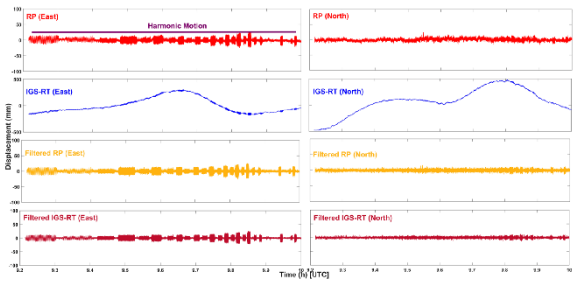

Figure 2. North and East time series for GPS-based solutions.

Case 3 was chosen as a representative example to examine the performance of the RT SF-PPP in capturing harmonic oscillations and compare it to the reference LVDT and RP. Figure 3 illustrates Case 3 for GPS-based solutions and LVDT, which shows the LVDT, filtered and unfiltered SF-RP, and SF-PPP-derived displacement, as well as their corresponding FFT spectrums. It is obvious that the low frequency components in the time series of the SF RT-PPP' time series disappear once the filter is applied. The effectiveness of the applied filtering is obviously seen when comparing the unfiltered and filtered time series of SF RT-PPP. Figure 3 illustrates that the RT SF-PPP-derived displacements agree well with the LVDT and SF-RP-derived displacements. The peak frequency and amplitude corresponding to the peak frequency remained stable before and after the filtering process for all GPS-based solutions.

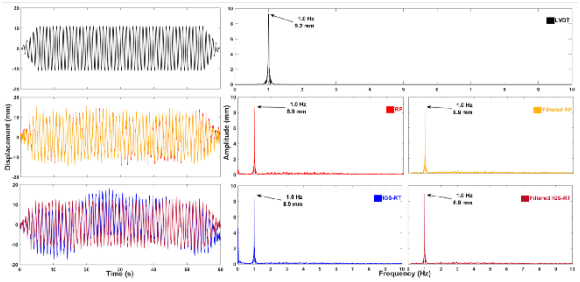

Figure 3. Time series (left) and corresponding FFT spectrums (right) for LVT, RP and SF-PPP.

Table 2 summarizes the detected peak frequency and corresponding amplitude obtained from all sensors discussed in the study for all harmonic oscillation cases. Values indicate unfiltered outcomes, whereas values in square brackets ([]) represent filtered results. The oscillation frequencies obtained by the LVDT, SF-RP, and SF RT-PPP solutions for all cases are in good agreement, as shown in the table. The filtered and unfiltered GPS-based methods performed similarly in determining the amplitudes corresponding to the peak frequencies. However, there are slight differences with LVDT. The differences of detected amplitude between SF RT-PPP and LVDT vary between 0 mm and 0.6 mm, whereas the differences for SF-RP vary between 0 .1 mm and 0.4 mm. This indicates that the SF RT-PPP is a powerful tool for structural health monitoring applications and the natural frequency of structures can be detected with low-cost GNSS receivers in real-time.

Table 2. The detected frequency and amplitude from all sensors

Case	LVDT		Relative Positioning		IGS Real Time PPP	
	Freq. [Hz]	Amp. [mm]	Freq. [Hz]	Amp. [mm]	Freq. [Hz]	Amp. [mm]
1	0.1	10.0	0.1	10.4 [10.1]	0.1	10.4 [10.1]
2	0.6	9.5	0.6	9.9 [9.9]	0.6	10.0 [10.1]
3	1.0	9.3	1.0	8.9 [8.9]	1.0	8.9 [8.9]
4	2.0	11.4	2.0	11.6 [11.6]	2.0	11.1 [11.1]
5	3.0	11.4	3.0	11.3 [11.3]	3.0	11.4 [11.3]

The maximum and RMSE (Root Mean Square Error) values of difference between LVDT and GPS-based techniques for all designed cases were computed to

investigate the performance of SF RT-PPP in detecting dynamic displacements and compare with the reference sensor LVDT, and results are given in Table 3. Values in square brackets are filtered results, whereas others refer to unfiltered. The maximum and RMSE values were significantly reduced after filtering, as seen in the table. Maximum values after filtering show an improvement of between 33% and 69% for IGS-RT based SF-PPP**.** According to the table, SF-RP has the smallest RMSE values for all events, varying between 1.7 and 5.2 mm, considering the unfiltered raw findings. Moreover, the RMSE values of differences from the LVDT of the raw solutions obtained from SF RT-PPP show slightly worse performance for all cases. However, it is obvious that after filtering, this performance improves significantly. While an average of 46% improvement was reached in all cases following the filtering process, it is obvious that improvements ranging from 46% to 84% were achieved. This finding demonstrates that the performance of RT SF PPP in determining dynamic displacements after applying a high-pass filter is comparable to that of the SF-RP, and SF-PPP provides a high potential for short-term dynamic behavior monitoring applications.

Table 3. Maximum and RMSE values of difference between LVDT and GPS-based methods

Case	Relative Positioning		IGS Real Time	
	Max [mm]	RMSE [mm]	Max [mm]	RMSE [mm]
1	8.7 [7.8]	1.7 [1.5]	22.9 [7.0]	8.5 [1.4]
2	13.3 [11.0]	2.9 [2.6]	13.2 [8.1]	4.4 [2.2]
3	8.3 [8.6]	2.1 [2.0]	10.5 [8.3]	3.7 [1.5]
4	12.5 [11.7]	3.9 [3.8]	13.1 [11.2]	4.3 [3.5]
5	16.6 [16.3]	5.2 [5.1]	17.7 [14.0]	5.6 [4.6]

IV. Conclusion

The performance of SF-PPP, which reduces measurement costs, and RT products are investigated in this study. A shake table was used to simulate 5 harmonic oscillation tests reflecting the natural behavior of engineering structures in the study. In the time and frequency domains, the SF RT-PPP approaches were compared to the LVDT sensor and the SF-RP. The findings of the frequency domain harmonic oscillation experiment reveal that the high-rate SF RT-PPP is comparable to SF-RP and has good agreement with LVDT. These frequency domain analyses indicate that oscillation frequencies of structures may be estimated effectively employing a single-frequency receiver and real-time products. Furthermore, given that the amplitude values corresponding to the peak frequency detected in SF RT-PPP solutions for all cases, there was no error higher than 0.5 mm. However, it was concluded that SF-PPP results require filtering in the time domain analysis. As a result, all GNSS-based approaches' time series were filtered using a fifth-order Butterworth high-pass filter to reduce long-term components. The RMSE and maximum error values improved significantly after the apply high-pass filter. The results of this study reveal that in structural health monitoring applications, the SF-PPP approach is as effective as the relative positioning method. Furthermore, this research demonstrates the SF-PPP approach may provide accurate and reliable displacement information when high pass filtering is used. This means that when structural health monitoring and early warning systems are operated with single frequency receivers, the SF-PPP approach provides reliable results, and real-time products are as accurate as final products in capturing short-term dynamic motions.

V. Acknowledgements

This work was supported by the Research Fund of the Gebze Technical University, Project Number: 2020-A-102-20.

References

Alcay, S., S. Ogutcu, I. Kalayci, and C.O. Yigit, (2019). Displacement monitoring performance of relative positioning and Precise Point Positioning (PPP) methods using simulation apparatus. *Advances in Space Research*, 63, pp. 1697-1707.

Avallone, A.M. Marzario, A. Cirella, A. Piatanesi, A. Rovelli, C. Di Alessandro, E. D'Anastasio, N. D'Agostino, R. Giuliani, and M. Mattone, (2011). Very high rate (10 Hz) GPS seismology for moderate-magnitude earthquakes: the case of the Mw 6.3 L'Aquila (central Italy) event. *J Geophys Res*, 116, pp. 1–14.

Bahadur, B. (2021). Real-time single-frequency precise positioning with Galileo satellites. *The Journal of Navigation*, 21(1), pp. 1-17.

Calais, E., J.Y. Han, C. Demets, and J.M. Nocquet, (2006). Deformation of the North American plate interior from a decade of continuous GPS measurements. *J Geophys Res*, 111, pp. 1–23.

Chen, L., Q. Zhao, Z. Hu, X. Jiang, C. Geng, M. Ge, and C. Shi (2018). GNSS global real-time augmentation positioning ,Real-time precise satellite clock estimation, prototype system construction and performance analysis. *Advances in Space Research*, 61 (1), pp. 367–384.

Defraigne, P., W. Aerts, and E. Pottiaux, (2015). Monitoring of UTC(k)'s using PPP and IGS real-time products. *GPS Solutions*, 19 (1), pp. 165–172.

El-Mowafy, A., M. Deo, and N. Kubo, (2017). Maintaining real-time precise point positioning during outages of orbit and clock corrections. *GPS Solution*, 21, pp. 937-947.

Ibáñez D., A. Rovira-García, J. Sanz, J.M. Juan, G. Gonzalez-Casado, D. Jimenez-Baños, C. López-Echazarreta, and I. Lapin, (2018). The GNSS Laboratory Tool Suite (gLAB) updates: SBAS, DGNSS and Global Monitoring System. *9th ESA Workshop on Satellite Navigation Technologies (NAVITEC 2018)*, Noordwijk, The Netherlands. December 5 - 7.

Kaloop R.M., C.O. Yigit, A. El-Mowafy, A.A. Dindar, M. Bezcioglu M., and J.H. Hu, (2020). Hybrid Wavelet and Principal Component Analyses Approach for Extracting

Dynamic Motion Characteristics from Displacement Series Derived from Multipath-affected High-rate GNSS Observations. *Remote Sensing*, 12(1):79

Kaloop, M.R., C.O. Yigit, and J.H. Hu, (2018). Analysis of the dynamic behavior of structures using the high-rate GNSS-PPP method combined with a wavelet-neural model: Numerical simulation and experimental tests. *Adv. Space Res*, 61, pp. 1512-1524.

Kouba, J. (2003). Measuring seismic waves induced by large earthquakes with GPS. *Stud Geophys Geod*, 47, pp. 741–755.

Kouba, J., and P. Héroux, (2001). Precise Point Positioning using IGS orbit and clock products. *GPS Solution*, 5, pp. 12–28.

Moschas, F., A. Avallone, V. Saltogianni, and S.C. Stiros, (2014). Strong motion displacement waveforms using 10-Hz precise point positioning GPS: an assessment based on free oscillation experiments. *Earthquake Eng Struct Dyn*, 43, pp. 1853–1866.

Savage, J.C., W. Gan, W.H. Prescott, and J.L. Svarc, (2004). Strain accumulation across the coast ranges at the latitude of San Francisco, 1994–2000. *J Geophys Res*, 109, pp. 1–11.

Takasu, T., and A. Yasuda, (2009). Development of the low-cost RTK-GPS receiver with an open-source program package RTKLIB. In: *International Symposium on GPS/GNSS, Seogwipo-si Jungmundong*, Korea, November 4–6.

Tang, X., G.W. Roberts, X. Li, and C. Hancock, (2017). Real-time kinematic PPP GPS for structure monitoring applied on the Severn suspension bridge, UK. *Adv. Space Res*, 60, pp. 925–937.

Wang, Z., Z. Li, L. Wang, X. Wang, and H. Yuan, (2018a) Assessment of multiple GNSS real-Time SSR products from different analysis centers. *ISPRS International Journal of Geo-Information*, 7 (3).

Wang, L., Z. Li, M. Ge, F. Neitzel, Z. Wang, and H. Yuan, (2018b) Validation and assessment of multi-GNSS real-time precise point positioning in simulated kinematic mode using IGS real-time service. *Remote Sensing*, 10 (2).

Xu, P., C. Shi, R. Fang, J. Liu, X. Niu, Q. Zhang, and T. Yanagidani, (2013). High-rate precise point positioning (PPP) to measure seismic wave motions: an experimental comparison of GPS PPP with inertial measurement units. *J Geod*, 87, pp. 361–372.

Yigit, C.O. (2016). Experimental assessment of post processed kinematic precise point positioning method for structural health monitoring. *Geomat Nat Hazards Risk*, 7, pp. 363–380

Yigit, C.O., A. El-Mowafy, A.A. Dindar, M. Bezcioglu, and I. Tiryakioglu, (2021). Investigating Performance of High-Rate GNSS-PPP and PPP-AR for Structural Health Monitoring: Dynamic Tests on Shake Table, *Journal of Surveying Engineering,* 147(1): 05020011:1-14.

Yigit, C.O., A. El-Mowafy, M. Bezcioglu, and A.A. Dindar, (2020) Investigating the effects of ultra-rapid, rapid vs. final precise orbit and clock products on high-rate GNSS-PPP for capturing dynamic displacements. *Structural Engineering and Mechanics*, 73(4), pp. 427-436.

Yigit, C.O., and E. Gurlek, (2017). Experimental testing of high-rate GNSS precise point positioning (PPP) method for detecting dynamic vertical displacement response of engineering structures. *Geomat Nat. Haz. Risk*, 8, pp. 893-904.

Yigit, C.O., M.Z. Coskun, H. Yavasoglu, A. Arslan, and Y. Kalkan, (2016). The potential of GPS Precise Point Positioning Method for Point Displacement Monitoring: A Case Study, *Measurement*, 91, pp. 398-404.

Yigit, C.O., A. El-Mowafy, A.A. Dindar, M. Bezcioglu, and I. Tiryakioglu, (2021). Investigating Performance of High-Rate GNSS-PPP and PPP-AR for Structural Health Monitoring: Dynamic Tests on Shake Table, *Journal of Surveying Engineering*, 147(1).

Zumberge, J.F., M.B. Heflin, D.C. Jefferson, M.M. Watkins, and F.H. Webb, (1997). Precise Point Positioning for the efficient and robust analysis of GPS data from large networks. *J Geophys Res*, 102, pp. 5005–5017.